

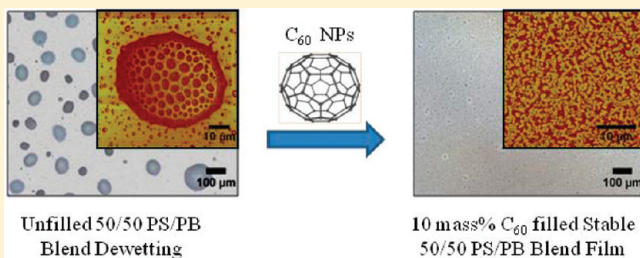
# Influence of C<sub>60</sub> Nanoparticles on the Stability and Morphology of Miscible Polymer Blend Films

Diya Bandyopadhyay,<sup>†</sup> Jack F. Douglas,<sup>‡</sup> and Alamgir Karim<sup>\*,†</sup>

<sup>†</sup>Department of Polymer Engineering, The University of Akron, Akron, Ohio 44325, United States

<sup>‡</sup>Polymers Division, National Institute of Standards and Technology, Gaithersburg, Maryland 20899, United States

**ABSTRACT:** We investigate the influence of fullerene (C<sub>60</sub>) nanoparticle (NP) additives on a thermodynamically miscible polymer blend thin film of polystyrene (PS) and polybutadiene (PB). In this system both homopolymer components individually dewet from the commonly used silicon substrate. Three NP concentration regimes having distinct blend nanocomposite film morphologies are observed: (a) In the neat blend and low NP mass (0–1%) range, the blend films rapidly dewet, apparently due to fluctuations in the polymer surface tension arising from the composition fluctuations of a surface enrichment layer at the film air boundary. This behavior is in sharp contrast to the corresponding NP-filled homopolymer films where dewetting is progressively slowed by the segregation of NPs to the solid substrate in this same concentration range. (b) In the intermediate NP concentration range of 1–5 mass %, the C<sub>60</sub> additive acts as a “compatibilizing agent”, progressively reducing the size of the dewetted droplets with increasing NP concentration. Dewetting is *fully suppressed* in the homopolymer films in this NP concentration range. We conclude that C<sub>60</sub> segregation to polymeric interfaces within blend film competes with the NP film stabilizing effect. (c) At higher NP concentrations between 5 and 10 mass %, the NPs enrich the substrate sufficiently to fully inhibit the blend film dewetting through a percolating blend–NP structure. At very high NP concentrations (10–15 mass %), the NPs form clusters within the blend film giving rise to a “spinodal clustering” NP morphology.



## INTRODUCTION

Polymer thin films are proving to be increasingly important because of their indispensable role in applications such as optoelectronic coatings, polymer-based bulk heterojunctions, nanolithography, biomedical scaffolds, and sensors.<sup>1,2</sup> Polymer blend thin films in particular have many practical applications due to their potential for combining different homopolymer attributes to create molecular composite materials, e.g., the combination of glassy and rubbery polymers to create tough structural materials, films of variable gas permeability, and conducting and insulating polymers of variable thermal and electrical conductivity. A persistent concern with blend films, however, as in homopolymer films, is their stability against dewetting.

While there are some previous studies of polymer dewetting on polymer substrates,<sup>3–5</sup> there has been limited investigation of the dewetting of polymer blend films on inorganic substrates where a coupling between dewetting and phase separation can make the interpretation of such measurements difficult. However, the escalating use of nanoparticles (NPs) such as C<sub>60</sub> as fillers in polymer films for diverse applications such as organic photovoltaic heterojunctions<sup>6</sup> makes the study of the stability of these complex nanocomposite films timely. Apart from issues relating to phase separation in these multicomponent films, there is also concern about the influence of NPs on the stability of the films against dewetting. The present paper focuses on this technologically important problem.

Almost a decade ago, Barnes et al.<sup>7</sup> demonstrated an unconventional route for controlling the dewetting of homopolymer films on nonwetable substrates that involved the addition of a small quantity (on the order of 1 mass %) of fullerene NPs (C<sub>60</sub>) to homopolymer films. The C<sub>60</sub> NPs were found to segregate to the film–substrate interface. This NP segregation modifies the polymer–substrate interaction<sup>8–13</sup> and also enhances film stability by pinning the growing contact lines of any dewetting holes that might form in the film.<sup>7</sup> A synergy between these thermodynamic and kinetic stabilization effects results in a strong and practically useful net film stabilization against dewetting. This phenomenon has been found to be very robust for other NP polymer thin film systems and suitable for the practical purpose of stabilizing films used in sensor applications.<sup>14</sup> This is uniquely a NP effect since larger particles behave like “dust” and lead to a prevalent tendency toward film dewetting. At the time of its discovery,<sup>7</sup> the NP film stabilization effect in homopolymers was completely unexpected.

In the present work, we explore an extension of Barnes et al.<sup>7</sup> to a binary miscible polymer blend system. Here, we systematically investigate the effects of addition of fullerene additives to a model blend film system of polystyrene (PS) and polybutadiene

Received: May 26, 2011

Revised: August 8, 2011

Published: September 28, 2011

(PB). Our initial study is constrained to the *one-phase region* of bulk blend miscibility in order to compare the film stabilization effect for the blends to the homopolymer films. We find again some intriguing effects of the NP additive associated in these films with the capacity of the NPs to preferentially segregate to new interfaces than the solid film–substrate interface.

By comparison, the effect of nanoparticles on even the simplest multicomponent (binary) blend film structure and stability is substantially more complex than homopolymer films due to simultaneous effects of polymer and particle segregation and dewetting. The phase stability of the film can be designed by the choice of molecular mass of the polymers and temperature to be in the single phase state. In this single phase region for the blend, surface segregation of the lower surface energy component occurs near the air surface for thin films and interfacial tension controls the segregation at the substrate boundary.<sup>15</sup> In the two-phase region, these segregation layers transform into wetting layers which serve to drive the polymer component segregation in their own fashion. There are evidently multiple phases accessible and multiple interfaces to which the NP can segregate, depending on the thermodynamic state of the film and its surroundings. In our initial study, we confine ourselves to the relatively simple case of thin blend films with NP in the single phase miscibility region of the blend phase diagram.

Naively, one might expect such “miscible” films to behave much like homopolymer films with NPs, but this proves not to be the case generally. Instead, we observe a partitioning of the  $C_{60}$  particles to the solid substrate (silicon wafer) that is strongly influenced by the segregation of the lower surface energy polymer to the air boundary, which in turn leads to a segregation of  $C_{60}$  to this interfacial region. We find that this competitive NP segregation process with the segregation of the NPs to the polymer enrichment layer interface greatly diminishes the NP stabilization effect observed in homopolymer films of which our blends are composed. Moreover, the interfacial segregation of the  $C_{60}$  to the polymer–polymer interface within the film largely influences the late-stage evolution of the morphology of the dewetting polymer films. Once the interfacial layer between the polymers is saturated with fullerene particles, substantial NP enrichment occurs at the solid substrate, and we finally see an effective stabilization effect against blend film dewetting, as seen before in the reference homopolymer films. These observations should help in future efforts in the design of stable nanocomposite blend films for diverse applications.

## EXPERIMENTAL SECTION

Polystyrene (PS), average relative molecular mass  $M_w = 3000$  g/mol and a polydispersity index (ratio of mass average to number-average relative molecular mass,  $M_w/M_n$ ) of 1.09, and polybutadiene (PB),  $M_w = 2400$  g/mol and a polydispersity index of 1.05, from Polymer Source Inc.<sup>16</sup> were used for our experiments. The molecular masses were chosen so as to be similar to the ones used in a previous homopolymer–NP study.<sup>7</sup> Laboratory grade toluene was used as the solvent for the polymers and was purchased from BDH Chemicals.<sup>16</sup> Homopolymer solutions of PS and PB in toluene were prepared separately by stirring the polymers in the solvent overnight. Blend solutions were made by dissolving the PS and PB in common solvent toluene, such that the total polymer concentration in the solvent was 3 mass %, and the solutions were then stirred overnight. Both homopolymer and blend solutions were filtered thoroughly using a  $0.2\ \mu\text{m}$  PTFE filter.  $C_{60}$  NPs of purity >99%, from Sigma-Aldrich Chemical Co.,<sup>16</sup> were dispersed in toluene, accompanied by ultrasonication, before addition to the blend

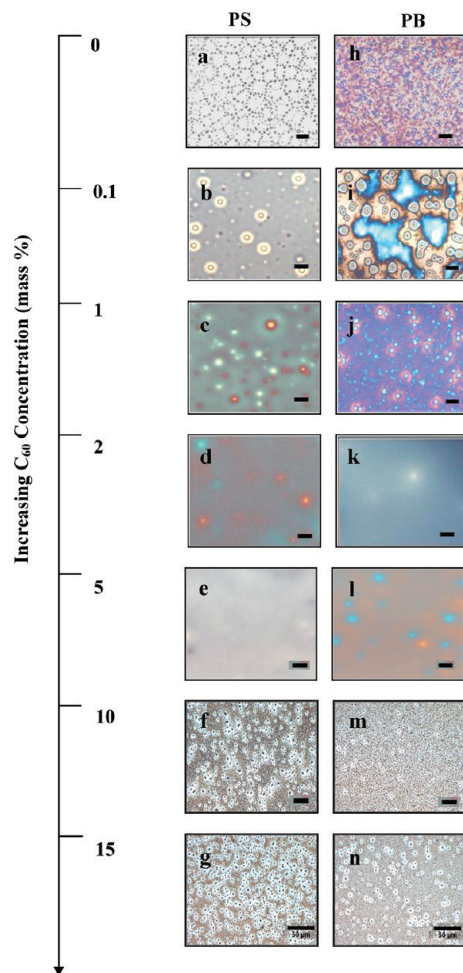


**Figure 1.** Optical microscope images tracking the homopolymer PS and PB thin film stability, annealed at 130 °C, as a function of  $C_{60}$  nanoparticle concentration: (a) neat homopolymer PS, (b) 0.1 mass %  $C_{60}$ -filled PS, (c) 1 mass %  $C_{60}$ -filled PS, (d) 2 mass %  $C_{60}$ -filled PS, (e) 5 mass %  $C_{60}$ -filled PS, (f) 10 mass %  $C_{60}$ -filled PS, (g) neat homopolymer PB, (h) 0.1 mass %  $C_{60}$ -filled PB, (i) 1 mass %  $C_{60}$ -filled PB, (j) 2 mass %  $C_{60}$ -filled PB, (k) 5 mass %  $C_{60}$ -filled PB, and (l) 10 mass %  $C_{60}$ -filled PB.

solution. The nanoparticle solutions were handled inside a nitrogen-purged glovebag.

A series of NP-filled blend solutions consisting of  $C_{60}$  concentrations varying from 0 to 10 mass % relative to total polymer blend weight were prepared by dissolving the  $C_{60}$ –toluene mixture with the blend solutions. Thin homopolymer and blend films were prepared by spin-coating at identical spin conditions of speed, acceleration, and time on nitrogen blow dried and UVO cleaned p-type Si (100) wafers purchased from Silicon Quest International.<sup>16</sup> This ensured that both homopolymer and blend films had the same thickness of  $110 \pm 2$  nm, which was verified using a DI-Veeco Nanoscope V atomic force microscope (AFM) and a Filmetrics F20-UV thin film analyzer. Annealing temperatures were kept in the one-phase region of bulk phase miscibility of this blend system as characterized by light microscopy in bulk films previously.<sup>17</sup> Blend film compositions in this study were kept fixed at 50:50 PS:PB composition. The upper critical solution temperature (UCST) in neat bulk PS/PB blend films was determined to be at 110 °C at a critical composition of 0.5.<sup>17</sup> The films were annealed at 130 °C, i.e., in the blend bulk one-phase region, for 1, 2, 12, and 48 h under vacuum. We observed that beyond 2 h the morphology and film stability remained unchanged, and

hence in all our further studies we chose to analyze and present sample data for an annealing time of 2 h. In parallel, we examined the stabilization effect of the  $C_{60}$  under similar conditions on each of the blend component homopolymer films as well as compared with our previous homopolymer dewetting stabilization by NP studies. The annealed blend and homopolymer films filled with NP were characterized using an Olympus BX41 optical microscope and a DI-Veeco Nanoscope V atomic force microscope (AFM).<sup>16</sup> Further, a Zeiss confocal laser fluorescence microscope<sup>16</sup> was used in order to map out the z-stacking distribution of  $C_{60}$  in the samples. Image J (NIH) data analysis software was used to quantify our results.

## RESULTS AND DISCUSSION

**$C_{60}$ -Filled Homopolymer Films.** Consistent with prior observations, neat PS and PB homopolymer thin films cast on silicon substrates spontaneously dewet on annealing above their glass transition temperatures and exhibit typical dewetting patterns as shown in optical microscopy (OM) images in Figures 1a and 1h, respectively. On adding fullerene nanoparticles (0.1–2 mass %), the dewetting holes are pinned progressively as observed before<sup>7</sup> (as shown in OM images in Figures 1b, c,i,j), and this phenomenon is now well-attributed to a fullerene surface enrichment layer on the substrate.<sup>7,13,14</sup> In the fullerene concentration range of 2–5 mass %, PS and PB homopolymer thin films are entirely stabilized against dewetting (Figures 1d,e,k,l). At even higher concentrations of  $C_{60}$  in the range of 10–15 mass % relative to PS and PB, we observe a large scale clustering of the  $C_{60}$  in the NP stabilized films (Figures 1f,g,m,n), a morphology that Cabral et al.<sup>18</sup> termed “spinodal clustering” in homopolymer PS films with  $C_{60}$ . Thus, all of our results on  $C_{60}$  addition to homopolymer films are consistent with literature studies.

**$C_{60}$  Nanoparticle-Induced Blend Film Morphology Regimes.** In the case of a (unfilled) PS/PB blend thin film, we observe a more complex and interesting behavior. In this study, all blend films are at critical bulk composition annealed in the single-phase region of the PS:PB bulk phase diagram. First, the dewetting occurs far more rapidly so than their homopolymer counterparts, and the film breaks up into droplets almost instantaneously. We suggest that this enhanced instability is due to polymer composition fluctuations in the surface enrichment layer that accelerate the film breakup process. Second, we observe a randomly dispersed bimodal distribution of large and small droplets rather than the traditional cellular-shaped Voronoi tessellation patterns (e.g., see Figure 1a)<sup>19</sup> in late-stage (occurs very fast however) film dewetting morphology of homopolymer films. Kinetic studies tracking film break up at as low as 30 s after annealing the film at 130 °C showed final stage dewetting, indicating a very fast film breakup process. The precise mechanism of this fast dewetting process of film breakup into final stage droplets requires further study using a high-speed camera, but this phenomenon is not the focus of our current study on nanoparticle-blend dewetting. Next, the effect on the bimodal distribution of dewet droplets with progressive addition of the NP initially causes the larger droplets to reduce in size, with a higher NP surface density, a NP-induced compatibilization “surfactant” effect. At higher NP concentrations, these larger droplets form percolating clusters composed of droplets having a bicontinuous morphology.<sup>20</sup> These dense NP-filled films appear optically homogeneous to the naked eye and at low magnification OM. Conspicuously, the NP concentrations ( $\approx 10$  mass %) required to stabilize the blend films against dewetting are well

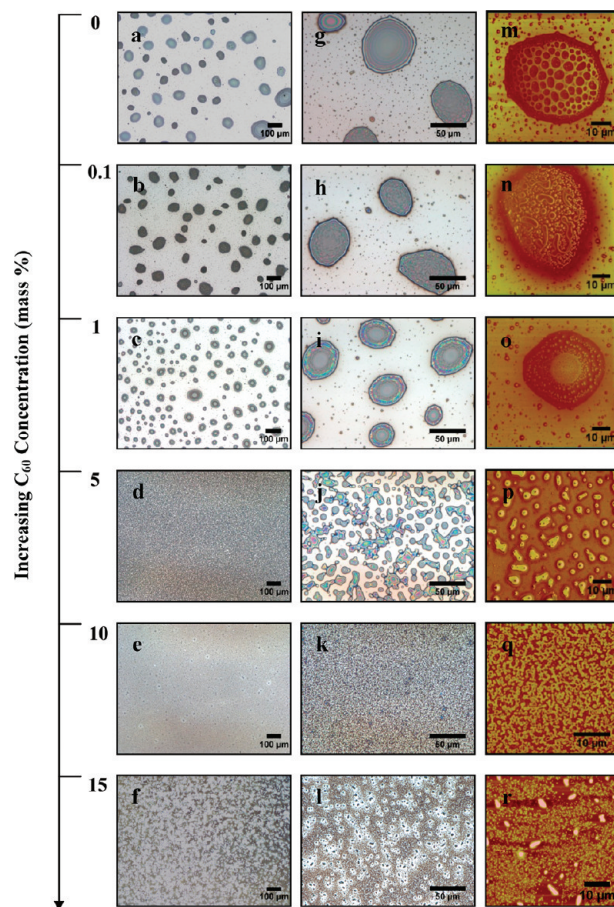


**Figure 2.** Morphological and film stability evolution as a function of  $C_{60}$  nanoparticle concentration in 50/50 PS/PB blend thin films annealed at 130 °C: (a–f) optical micrographs of neat, 0.1, 1, 5, 10, 15 mass %  $C_{60}$ -filled blend films, respectively; (g–l) optical micrographs of neat, 0.1, 1, 5, 10, 15 mass %  $C_{60}$ -filled blend films, respectively, at a higher magnification; (m–r) AFM phase images of neat, 0.1, 1, 5, 10, 15 mass %  $C_{60}$ -filled blend films, respectively.

above the threshold concentration ( $\approx 2$  mass %) needed to stabilize the individual homopolymer films against dewetting. In blend films, the NP-induced film stabilization is “recovered” at relatively higher NP concentrations ( $\approx 7$ –10 mass %) to stabilize the films in a fashion similar to the NP-filled homopolymer films. This is due to partitioning of the NP within the blend interfaces and the blend substrate interface. A neat critical composition PS/PB blend film cast on a silicon substrate exhibits evident dewetting almost immediately at 130 °C, 20 °C above the bulk  $T_c$  of 110 °C. While the macroscopic (large) dewet droplets look similar to those found in homopolymer dewetting, they are randomly distributed spatially, as illustrated in low- and high-magnification OM images in Figures 2a and 2g, respectively. Additionally, there are numerous tiny dewet droplets that are observable even by high-resolution optical microscopy. The droplet distribution for neat blends is distinctly bimodal, and an image analysis using Image J (Figure 3A) illustrates the droplet domain count and droplet size distribution versus mass concentration of nanoparticles as plotted in Figure 3B. A closer look at the microstructure of the large droplet reveals a single

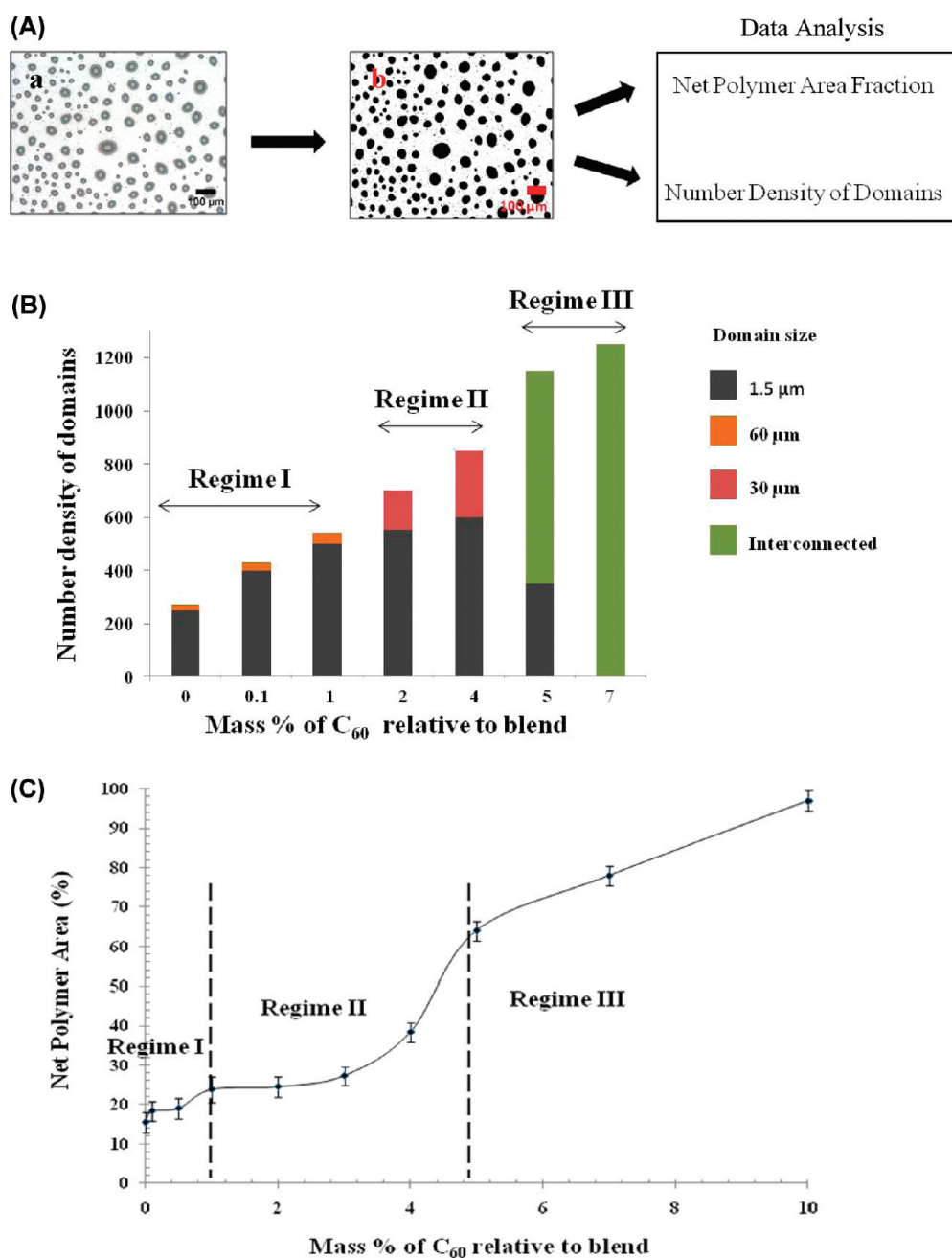


**Figure 3.** (A) Image analysis of a 1 mass %  $C_{60}$ -filled 50/50 PS/PB blend film annealed at 130 °C. (B) A plot of the number density of polymer blend dewet domains and domain size distribution as a function of  $C_{60}$  nanoparticles concentration. (C) A plot of net polymer blend film coverage on the substrate (a measure of film wetting and thus stability against dewetting) as a function of  $C_{60}$  nanoparticles concentration, indicating the three distinct regimes of film stability. The line (curve) interpolating between the points is drawn to guide the eye. Bars on data points indicate a standard uncertainty of  $\pm 2.5$  of the "% of net polymer area".

"moth-eye" type of morphology as shown in an AFM image in Figure 2m. This moth-eye morphology is apparently a manifestation of the dewetting induced capillary wave driven breakup of a surface enrichment layer of PB, which enriches the polymer-air interface by virtue of its lower surface energy ( $\approx 32$  mJ/m<sup>2</sup> for PB and 40.5 mJ/m<sup>2</sup> for PS).<sup>21,22</sup> The surface curvature of the dewetted blend film droplets imposes a tension on the surface enrichment cap layer that probably influences the breakup of this layer.

Next, Figures 2b,h show that the optically macroscopic dewetting morphology is only mildly impacted upon adding

0.1 mass % of  $C_{60}$  nanoparticles (NPs) to the polymer blend and shows a plot of domain number density and domain size as a function of NP concentration (Figure 3B). However, the surface layer breakup is appreciably affected by the addition of NPs, with the fullerenes apparently acting as surfactants at the surface enrichment layer interface. This leads to emulsion-like droplets that are elongated, but of smaller width and highly distorted in shape from a circular shape (Figure 2n). A core-shell type of morphology is observed upon further increasing the added NP concentration to 1 mass % (Figures 2c,i,o), with the NPs aiding

the coalescence of the surface enriched layer leading to a polymer “disc” at the top of the film forming a 2-D core–shell type of structure. The effect of the NPS on domain size and number density is indicated in Figure 3B. Evidently, the overall dewetting of the blend film on the silicon substrate is not affected much by the presence of NPs up to a concentration of  $\approx 1$  mass %, with the fullerenes only segregating to the polymer–polymer interface and thus affecting the morphology of the dewet droplets. We again emphasize that the blend films behaves rather differently from the individual homopolymer films in relation to the concentration of NP required for stabilization against dewetting. In the blend film case, little  $C_{60}$  segregation at the substrate is expected at such low concentrations due to the preferential partitioning of the NPs to the polymer–polymer interface as is later confirmed by selective solvent etching and confocal fluorescence microscopy.

A considerable suppression in the overall blend dewetting is observed at higher added NP concentrations as shown in Figures 2d,j,e,k,f,l for 5, 10, and 15 mass % of  $C_{60}$ , respectively, and the domain size distribution for 5% is almost homogenized (Figure 2p) or unimodal (Figure 3B). After reaching a saturation concentration at the polymer–polymer interface, the NPs begin to segregate to the substrate as seen in the subsequent internal morphology analysis section as well as in previously studied PS- $C_{60}$  nanocomposite thin film systems using direct techniques like neutron reflectivity measurements.<sup>13</sup> At a NP concentration of 10 mass %, we obtain a bicontinuous interconnected PS/PB blend film morphology, as shown in Figure 2q. With a further increase in NP concentrations, however, the in-plane morphology gradually becomes rougher and the 15 mass %  $C_{60}$ -PS/PB blend film exhibits a “spinodal clustering” pattern of the  $C_{60}$  NPs (Figure 2r). This phenomenon of spinodal clustering of  $C_{60}$  NPs at high concentrations has been recently quantified extensively by Cabral et al.<sup>18</sup> for homopolymer PS- $C_{60}$  thin films, although these structures require higher  $C_{60}$  concentrations (typically 7–10 mass %) in the homopolymer films. This further emphasizes the concentration “lag” in morphology and stability development in blend films as compared to homopolymer films arising from the competitive NP segregation to polymer–polymer and polymer–substrate interfaces.

**Discussion on  $C_{60}$  Nanoparticle-Induced Film Stabilization Regimes.** We now show that there are three distinct regimes of blend film stabilization as a function of NP concentration (Figures 3B,C).

**Regime I.** Regime I, at low  $C_{60}$  concentrations (0 mass % < NP concentration < 1 mass %), is characterized by complete dewetting of the blend film with dewet droplets exhibiting interesting “moth-eye”-like structures generated as a result of the uniform rupture of the surface enrichment layer of the lower surface energy polymer. The NP in this layer can be expected to influence the impact the coalescence of the droplets to form larger droplets as the films progressively dewet and an inhibition of this process should result in somewhat smaller droplets. Because of a preferential NP partitioning to the blend polymer–polymer interface versus polymer–substrate interface in regime I, there is no significant effect of the NPs on film stability against dewetting and a PS/PB blend film filled with  $C_{60}$  NPs up to a mass concentration of  $\approx 1\%$  relative to the blend dewets macroscopically.

**Regime II.** In regime II (1 mass % < NP concentration < 5 mass %), the PS/PB blend films continue to dewet the substrate. However, the net macroscopic polymer coverage begins to increase,

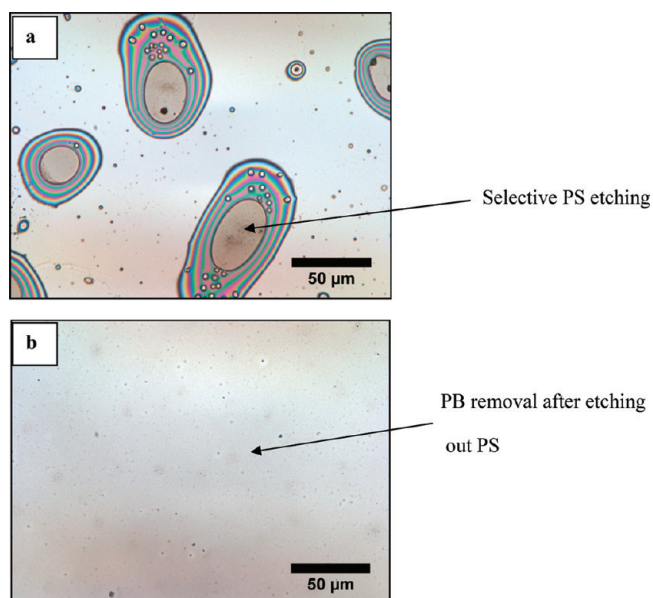


**Figure 4.** Qualitative composition analysis of neat 50/50 PS/PB blend thin film annealed at 130 °C via (a) selective solvent etching to remove PS and (b) further removal of PB with a PB selective solvent.

indicating an increased film stability. This is attributed to an onset of the  $C_{60}$  NPs segregating to the substrate, although to a smaller extent as compared to segregation to the polymer–polymer interface near the air boundary. Substrate segregation occurs in part due to an onset of saturation of the fullerenes at the polymer–polymer interface. As indicated in Figure 3B, a bimodal size distribution of the dewet droplets persists. This is attributed to an enhanced  $C_{60}$  segregation to the interface between the droplets. The  $C_{60}$  “surfactant” suppresses coalescence of the dewet drops to form larger domains as found in regime I, leading to a reduced dewet drop size (diameter  $\approx 30\ \mu\text{m}$ ). The polymer film morphology in this regime transforms from a 2-D core shell structure, to an interconnected network structure. Both the morphology and the area coverage studies indicate that at intermediate concentrations the fullerene concentration begins to become saturated near the polymer–polymer interface and the NP then start to segregate appreciably to the solid substrate.

**Regime III.** At relatively high  $C_{60}$  concentrations (5 mass % < NP concentration < 15 mass %) of regime III there is complete film stability yet the film has a microstructure so it is not spatially homogeneous. Up to a NP concentration of 10 mass %, the film morphology makes a transition from an interconnected film structure to a more continuous blend film by optical microscopy on the scale of micrometers and a highly structured morphology by atomic force microscopy imaging at a submicrometer scale. At these concentrations of NPs, we infer that the fullerene-rich polymer (likely PB) layer near the substrate forms a gel-like layer, thus modifying the substrate energy and structure. In this regime, the dewet droplet size distribution transforms from a discrete bimodal behavior to a uniform interconnected bicontinuous film morphology (Figure 3B), implying a significant suppression of coalescence between the polymer phases due to surfactant effects of the NPs, in addition to complete film stabilization via NP segregation to the substrate. At NP concentrations above 10 mass %, the NPs tend to form clusters giving rise to a spinodal blend–NP morphology.

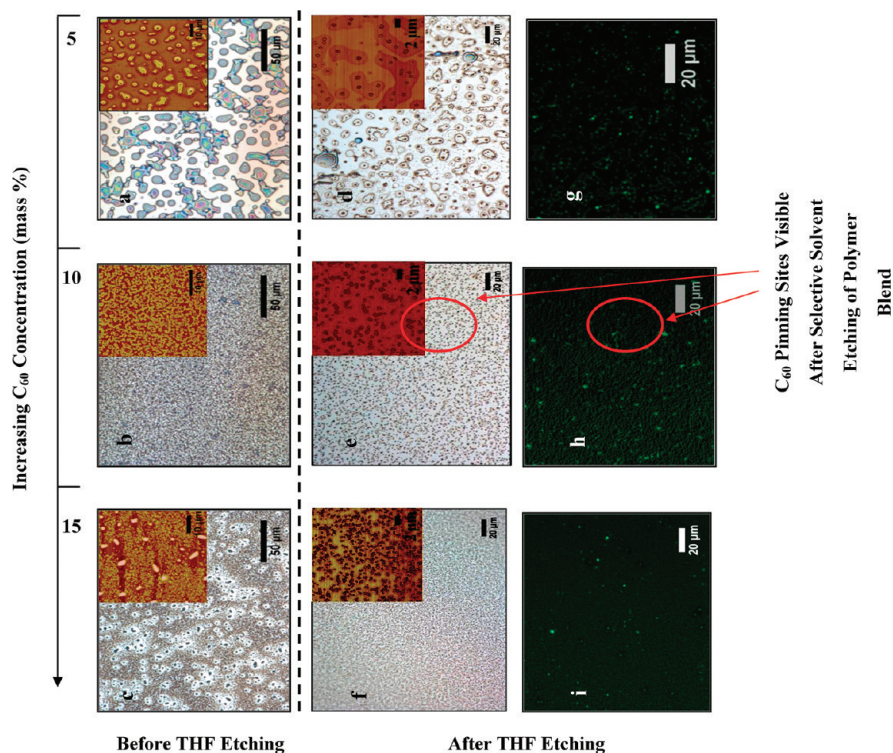


**Figure 5.** Internal morphology analysis of neat and NP-filled 50/50 PS/PB blend films annealed at 130 °C via selective solvent etching and confocal fluorescence microscopy: (a–c) optical micrographs of 5, 10, and 15 mass %  $C_{60}$ -filled blend films, respectively; (d–f) optical micrographs of 5, 10, and 15 mass %  $C_{60}$ -filled blend films, respectively, etched with THF (PS and PB selective) and showing remnant  $C_{60}$  pinning sites; (g–i) confocal fluorescence micrographs of 5, 10, and 15 mass %  $C_{60}$ -filled blend films, respectively, etched with THF.

**$C_{60}$  Nanoparticle-Induced Dewetting Pinning.** Selective solvent etching of the polymer blend dewet domains helps us to identify qualitatively the composition of the dewet droplets as shown in Figure 4 for a neat blend film annealed in the one-phase region. The central core is mainly PS-rich, whereas the shell is PB-rich, as seen from a PS selective solvent etch (Figure 4a) followed by selective removal of PB (Figure 4b). Further, selective solvent etching of the blend at  $C_{60}$  concentrations in the unstable and stable region of film wetting confirms our hypothesis of  $C_{60}$  induced stabilization via segregation to the substrate. After selectively removing the polymer blend, we observe NP aggregates on the silicon surface that correspond to the NP “pinning sites” that retard film dewetting. Confocal fluorescence microscopy corroborates these results further by exhibiting increased fluorescence signal (from  $C_{60}$ ) from the pinning sites on the substrate with increasing  $C_{60}$  concentration. Figures 5a,b,c show annealed (5, 10, and 15 mass %)  $C_{60}$ -filled blend films. Solvent-etched samples are shown in Figures 5d,e,f, from which we can see an increase in density of the substrate-segregated NPs. The AFM image insets of the corresponding optical micrographs exhibit these pinning sites clearly, and these sites are also highlighted by confocal fluorescence images in Figures 5g,h,i. Thus, selective polymer etching methods, as well as fluorescence microscopy, confirm the presence of  $C_{60}$  NPs at the silicon substrate and also indicate the increase in substrate coverage by  $C_{60}$  with increasing NP concentration. The fluorescence image of Figure 5a leads us to conclude that bimodally distributed dewet droplets contain all three components, namely PS, PB, and  $C_{60}$ , with the larger dewet droplets at lower  $C_{60}$  concentrations (<1 mass %) exhibiting a core–shell type of

structure. For a  $C_{60}$  concentration > 5 mass %, the blend film clearly develops an interconnected structure, and the confocal fluorescence images further suggest the presence of a polymer layer on top of a “gel-like”  $C_{60}$ -rich layer mentioned before. This layer screens the otherwise unfavorable interactions between the substrate and the polymer blend.<sup>7,13,23</sup> Neutron reflectivity studies were carried out to observe any NP layering below the stabilized polymer layer, but due to the high in-plane roughness of these dewetted film layers, no meaningful data for quantifying the NP segregation could be obtained.

## CONCLUSIONS

Our study of a model polymer blend annealed in the bulk single phase with a well-defined nanoparticle additive provides some general insights into the stability of nanocomposite blend films found in high impact technological applications. The stability trends with increasing nanoparticles concentration are significantly different from the homopolymer film counterparts, even when the blend film is miscible. In particular, the dewetting of blend films proceeds more rapidly compared to its homopolymer constituents, even without the nanoparticles. With a small concentration of nanoparticles, we observe a bimodal distribution of dewetted film droplets reflecting a “surfactant compatibilization” effect with increasing NP addition that progressively inhibits the droplet coalescence process necessary for forming large dewetted droplets. Finally, we observe a strong stabilization of PS/PB blend films by the addition of  $C_{60}$  nanoparticles at high concentrations of NP. We suggest that this occurs via the formation of a gel-like layer of fullerenes at the

silicon substrate that modifies the substrate–polymer interaction and pins the growth of dewetting holes, as in the case of homopolymer films at lower nanoparticle concentrations. We attribute this stark difference to the competitive segregation of the NPs, preferentially to a surface enrichment induced polymer–polymer interface and subsequently to the solid substrate at higher concentrations.

## AUTHOR INFORMATION

### Corresponding Author

\*Tel (330) 972-8324; e-mail alamgir@uakron.edu.

## ACKNOWLEDGMENT

This work was supported by the University of Akron Research Foundation (UARF), the U.S. Department of Energy (DOE-BES Grant DE-FG02-10ER4779), and the Austen BioInnovation Institute in Akron (ABIA)—supported Akron Functional Materials Center (AFMC). D.B. also thanks Dr. Manish M. Kulkarni, Dr. Jola Marszalek, Gurpreet Singh, and Prof. Matthew L. Becker for helpful discussions.

## REFERENCES

- (1) Licari, J. J. *Plastic Coatings for Electronics*; McGraw-Hill: New York, 1970.
- (2) Sariciftci, N. S.; Smilowitz, L.; Heeger, A. J.; Wudl, F. *Science* **1992**, 258, 1474.
- (3) Reiter, G. *Phys. Rev. Lett.* **1992**, 68, 75.
- (4) Sharma, S.; Rafailovich, M. H.; Peiffer, D.; Sokolov, J. *Nano Lett.* **2001**, 1, 511.
- (5) Chung, H.; Ohno, K.; Fukuda, T.; Composto, R. J. *Macromolecules* **2007**, 40, 384.
- (6) Chen, D.; Nakahara, A.; Wei, D.; Nordlund, D.; Russell, T. P. *Nano Lett.* **2011**, 11, 561.
- (7) Barnes, K. A.; Karim, A.; Douglas, J. F.; Nakatani, A. I.; Gruell, H.; Amis, E. J. *Macromolecules* **2000**, 33, 4177.
- (8) Krishnan, R. S.; Mackay, M. E.; Duxbury, P. M.; Pastor, A.; Hawker, C. J.; Van Horn, B.; Asokan, S.; Wong, M. S. *Nano Lett.* **2007**, 7, 484.
- (9) Luo, H.; Gersappe, D. *Macromolecules* **2004**, 37, 5792.
- (10) Hosaka, N.; Tanaka, K.; Otsuka, H.; Takahara, A. *Compos. Interfaces* **2004**, 11, 297.
- (11) Koo, J.; Shin, K.; Seo, Y. S.; Koga, T.; Park, S.; Satija, S.; Chen, X.; Yoon, K.; Hsiao, B. S.; Sokolov, J. C.; Rafailovich, M. H. *Macromolecules* **2007**, 40, 9510.
- (12) Lee, J. Y.; Buxton, G. A.; Balazs, A. C. *J. Chem. Phys.* **2004**, 121, 5531.
- (13) Han, J. T.; Lee, G.-W.; Kim, S.; Lee, H.-J.; Douglas, J. F.; Karim, A. *Nanotechnology* **2009**, 20 (1–6), 105705.
- (14) Holmes, M. A.; Mackay, M. E.; Giunta, R. K. *J. Nanopart. Res.* **2007**, 9, 753.
- (15) Grull, H.; Sung, L.; Karim, A.; Douglas, J. F.; Satija, S. K.; Hayashi, M.; Jinnai, H.; Hashimoto, T.; Han, C. C. *Europhys. Lett.* **2004**, 65, 671.
- (16) Certain commercial materials and instruments are identified in this article to adequately specify the experimental procedure. In no case does such identification imply recommendation or endorsement by the National Institute of Standards and Technology; nor does it imply that materials or equipment identified are necessarily the best available for the purposes.
- (17) Lin, J. L.; Rigby, D.; Roe, R. J. *Macromolecules* **1985**, 18, 1609.
- (18) Wong, H. C.; Cabral, J. T. *Phys. Rev. Lett.* **2010**, 105, 038301.
- (19) Reiter, G. *Phys. Rev. Lett.* **1992**, 68, 75. *Langmuir* **1993**, 9, 1344. *Macromolecules* **1994**, 27, 3046.
- (20) Sundararaj, U.; Macosko, C. W. *Macromolecules* **1995**, 28, 2647.

(21) Brandrup, J.; Immergut, E. H.; Grulke, E. A. *Polymer Handbook*; John Wiley & Sons: New York, 1999.

(22) van Krevelen, D. W.; Nijenhuis, K. T. *Properties of Polymers*, 4th ed.; Elsevier: Amsterdam, 2009.

(23) McGarrity, E. S.; Frischknecht, A. L.; Frink, L. J. D.; Mackay, M. E. *Phys. Rev. Lett.* **2007**, 99, 238302.